JOURNAL OF NANO- AND ELECTRONIC PHYSICS
Vol. **10** No 2, 02010(6pp) (2018)

ЖУРНАЛ НАНО- ТА ЕЛЕКТРОННОЇ ФІЗИКИ
Том **10** № 2, 02010(6cc) (2018)

Physical Adsorption of N-containing Heterocycles on Hexagonal Boron Nitride: DFT-D3 Study

I.K. Petrushenko*

Irkutsk National Research Technical University, 83, Lermontov Str., 664074 Irkutsk, Russia

(Received 11 January 2018; revised manuscript received 26 April 2018; published online 29 April 2018)

In this paper, the physical adsorption of five different N-containing organic heterocycle molecules and benzene on hexagonal boron nitride (*h*-BN) has been studied using dispersion-corrected density functional theory (DFT-D3). Adsorption energies (E_a) have been obtained for all studied molecules, and it has been shown that E_a for pyridazine is maximal one. Electronic properties of the molecule/*h*-BN complexes have also been obtained. DFT-D3 calculations show that all the studied molecules, except pyridazine, introduce only minor changes in the HOMO-LUMO gap of *h*-BN upon the physisorption. Thus, the physisorption of N-containing heterocycle molecules on the h-BN plane through noncovalent van der Waals interactions represents a simple method to add arbitrary functionality to *h*-BN, preserving its electronic properties undisturbed. Additionally, the comparison of E_a for the adsorption on graphene, *h*-BN and their hybrid structure has been made.

Keywords: DFT, Hexagonal boron nitride, Nitrogen, Heterocycle, Physisorption, Graphene.

DOI: 10.21272/jnep.10(2).02010

PACS numbers: 31.15.E –, 61.48.De, 68.43. – h, 68.43.Bc.

1. INTRODUCTION

Graphene, a monolayer of graphite, possesses valuable characteristics, such as high thermal conductivity, high mechanical stability, and unusual electronic properties [1]. The studies on graphene were followed by those on hexagonal boron nitride (*h*-BN), silicene, and other two-dimensional (2D) nanostructures [2-4]. H-BN is a one-layer material having distinct differences and advantages compared to the properties of its carbon counterpart as it exhibits polar character of the B-N bonds. Besides this, h-BN exhibits profound chemical and thermal stability, as well as high mechanical stiffness [5].

An effective technique which can help one to achieve the best performance for 2D nanomaterials-based devices is functionalization. In this respect, the vast literature exists on the growing applications of graphene and *h*-BN modified through both noncovalent interactions and covalent bonding. The former are of importance for most applications because, for example, the extended π-system of graphene-like materials is not interrupted, which means that useful properties such as electric conductivity or mechanical strength are not affected. In addition, the impermanent character of noncovalent interactions as well as relatively simple adsorption/desorption methods offer high flexibility in handling of the adsorbent.

Recently, adsorption of aromatic molecules on graphene has been extensively studied. The interaction between them is considered by scientists as a suitable model for the interaction between graphene layers [6]. At the same time, some aromatic molecules can also be used to tune-up the electronic structure of graphene [7, 8]. For example, Wuest and Rochefort have shown that aminotriazines are strongly adsorbed on graphite surface, whereas benzene and pyridine have moderate adsorption energies (E_a) [9]. Some authors believed that benzene and naphthalene molecules bind very weakly, or do not bind at all, to graphene sheets [10]. However, the works devoted to studies of noncovalent interactions between h-BN and heterocyclic molecules are rather scarce. Many questions are far from being solved.

In this paper, we present a dispersion-corrected density functional theory (DFT-D3) study on the physical adsorption of a series of five N-containing heterocyclic molecules on *h*-BN. The following compounds: pyridine (C_5H_5N), pyrazine (*para*-$C_4H_4N_2$), pyrimidine (*meta*-$C_4H_4N_2$), pyridazine (*ortho*-$C_4H_4N_2$), and 1,3,5-triazine ($C_3H_3N_3$) as well as benzene (C_6H_6), for the sake of comparison, are considered. Nitrogen heterocycles represent a highly important class of compounds which are widely used in materials science, agrochemistry, and medicinal chemistry. Considering pyridine as a precursor to pharmaceuticals [11], it is, therefore, important to study the binding mechanism of this molecule with nanosheets of *h*-BN.

Besides this, the aforementioned compounds are very interesting and convenient models for studying the noncovalent interactions. Indeed, one of the main components of van der Waals interactions is a dipole-dipole interaction. The existence of nitrogen atoms in the rings of the studied molecules leads to the electron density shift and, therefore, the induction of the dipole moment. The abundance of polar B-N bonds in *h*-BN can be regarded as the plenty of dipoles that may promote the interactions between the adsorbate and the adsorbent. The obtained results are likely to be useful for further theoretical and experimental studies on the noncovalent functionalization of *h*-BN.

2. COMPUTATIONAL METHODS

All the DFT-D3 calculations were carried out using Orca 4.0.1 program package [12]. The dispersion-corrected PBE-D3 functional [13-17] together with the SVP basis set [18] were employed. This functional has

---

* igor.petrushenko@istu.edu

been demonstrated to be reliable and commonly used in the studies of adsorption phenomena [19-21]. For all calculations, we involved default convergence criteria of Orca 4.0.1 for optimization.

As an *h*-BN model ($B_{12}N_{12}H_{12}$), we employed a coronene-based model ($C_{24}H_{12}$), in which we substitute all carbon atoms with boron and nitrogen in an alternate manner (Fig. 1).

The adsorption energy (E_a) of the studied molecules adsorbed on *h*-BN was calculated as:

$$E_a = E(\text{molecule}/h\text{-BN}) - E(\text{molecule}) - E(h\text{-BN}),$$

where E(molecule/*h*-BN), E(molecule), and E(*h*-BN) denote the total energies of the relaxed molecule/*h*-BN complex, the studied molecule, and *h*-BN, respectively. The negative E_a values denote the exothermic process. For all E_a, we made the basis set superposition error (BSSE) correction to eliminate the effect of basis set incompleteness by employing the counterpoise correction method. The equilibrium distance (R) is a normal length between the center of the molecular ring and the *h*-BN plane. Multiwfn program was used to obtain the density of states (DOS) plots [22].

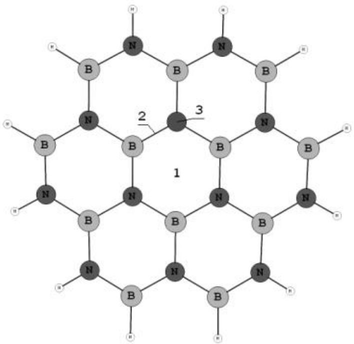

Fig. 1 – A $B_{12}N_{12}H_{12}$ model adopted in this study as *h*-BN. The initial adsorption positions are denoted as 1 ('hollow'), 2 ('bond'), 3 ('top'). Grey balls are boron, dark grey balls are nitrogen. Small balls are hydrogen

3. RESULTS AND DISCUSSIONS

In general, one can highlight only a few initial positions of possible sorption of studied molecules onto *h*-BN. They are 'hollow' (at the center of a hexagon ring), 'bond' (at the center of a respective bond), and 'top' (above a respective atom) (Fig. 1). We study all the positions of a benzene molecule and five heterocyclic molecules in respect to the *h*-BN surface as well as different distances between them. The equilibrium configurations for benzene as well as five heterocycles (pyridine (C_5H_5N), pyrazine (*para*-$C_4H_4N_2$), pyrimidine (*meta*-$C_4H_4N_2$), pyridazine (*ortho*-$C_4H_4N_2$), and 1,3,5-triazine ($C_3H_3N_3$)) physisorbed on h-BN are shown in Fig. 2. First, we turn to the benzene molecule, which is almost parallel to the *h*-BN plane (Fig. 2). For the N-containing heterocycles, we observe the slopes towards the *h*-BN. The centers of the aromatic rings are located above the nitrogen atom in the cases of benzene, pyrazine, pyridazine, and 1,3,5-triazine. The equilibrium distance (R) between the benzene molecule and the *h*-BN surface is 3.33 Å, E_a is – 0.304 eV. Fig. 2 shows electron density of the benzene/*h*-BN complex. The 0.2 isodensity model (red solid, middle; bottom) clearly shows that the preferential position of benzene adsorption is defined by the mutual distribution of the electron densities of the adsorbate and the adsorbent. Thus, the center of the benzene ring is above the local maximum of the electron density (the nitrogen atom) of *h*-BN. The carbon atoms of the benzene ring are located above the local minima of the electron density (boron atoms) (Fig. 2). We suppose that the mutual orientation of benzene and *h*-BN is due to the electrostatic interactions of their electron clouds.

Further, we study adsorption of five N-containing heterocyclic molecules on the *h*-BN surface. The calculated R, μ, and E_a values as well as charge transfers (Δc), and HOMO-LUMO gaps (E_g) are summarized in Table 1.

The adsorption of studied molecules does not lead to a distortion of an *h*-BN sheet or noticeable changes in lengths of the bonds underlying the adsorbed molecules. The variation of R depending on the molecule adsorbed is also only moderate (Table 1). These values are also close to the corresponding ones for the adsorption of other aromatic molecules on pristine graphene sheets and graphene-like boron nitride/carbon heterostructures (GBNCHs) [23, 24]. To get deeper insight into the structure-E_a relation, we consider the overall interaction energy $\varphi(z)$ of a molecule at a distance z from a surface. It can be represented by the following expression [25]:

$$\varphi(z) = \varphi_D + \varphi_R + \varphi_P + \varphi_{F_\mu} + \varphi_{FQ},$$

where φ_D and φ_R represent attractive and repulsive energies, respectively; φ_P, φ_{F_μ}, and φ_{FQ} are energies of polarization, field-dipole, and field gradient-quadrupole interactions, respectively. The non-specific terms (φ_D and φ_R) are always present, whereas electrostatic energies existence (φ_P, φ_{F_μ}, and φ_{FQ}) depends on the nature of the adsorbate and/or adsorbent. Whereas some symmetrical heterocycles, pyrazine and 1,3,5-triazine, exhibit zero dipole moments, the non-symmetrical mutual positions of C and N atoms leads to the increase in μ values for the rest heterocycles (Table 1). Thus, the φ_P term is valid for all studied molecules as the B-N bonds in *h*-BN exhibit polar nature. The φ_{F_μ} term is a feature of only 3 molecules: pyridazine, pyridine, and pyrimidine. Therefore, the latter three molecules are characterized by the larger (more negative) E_a values among studied heterocycles. Pyrazine and 1,3,5-triazine, in turn, have the minimal E_a values.

It is of use to compare the results of the present study with those on the adsorption on graphene and GBNCHs, which combine graphene and *h*-BN moieties in one sheet [23]. In this paper and elsewhere, various calculation methods used, therefore, we can not directly compare the results on *h*-BN and graphene. We can rather compare the trends of their changes. Alternatively, there is a possibility for direct comparison of data on *h*-BN and GBNCHs.

First, we take into consideration the physisorption on graphene. Using a number of dispersion-corrected functionals, Ramos-Berdullas et al. obtained the following

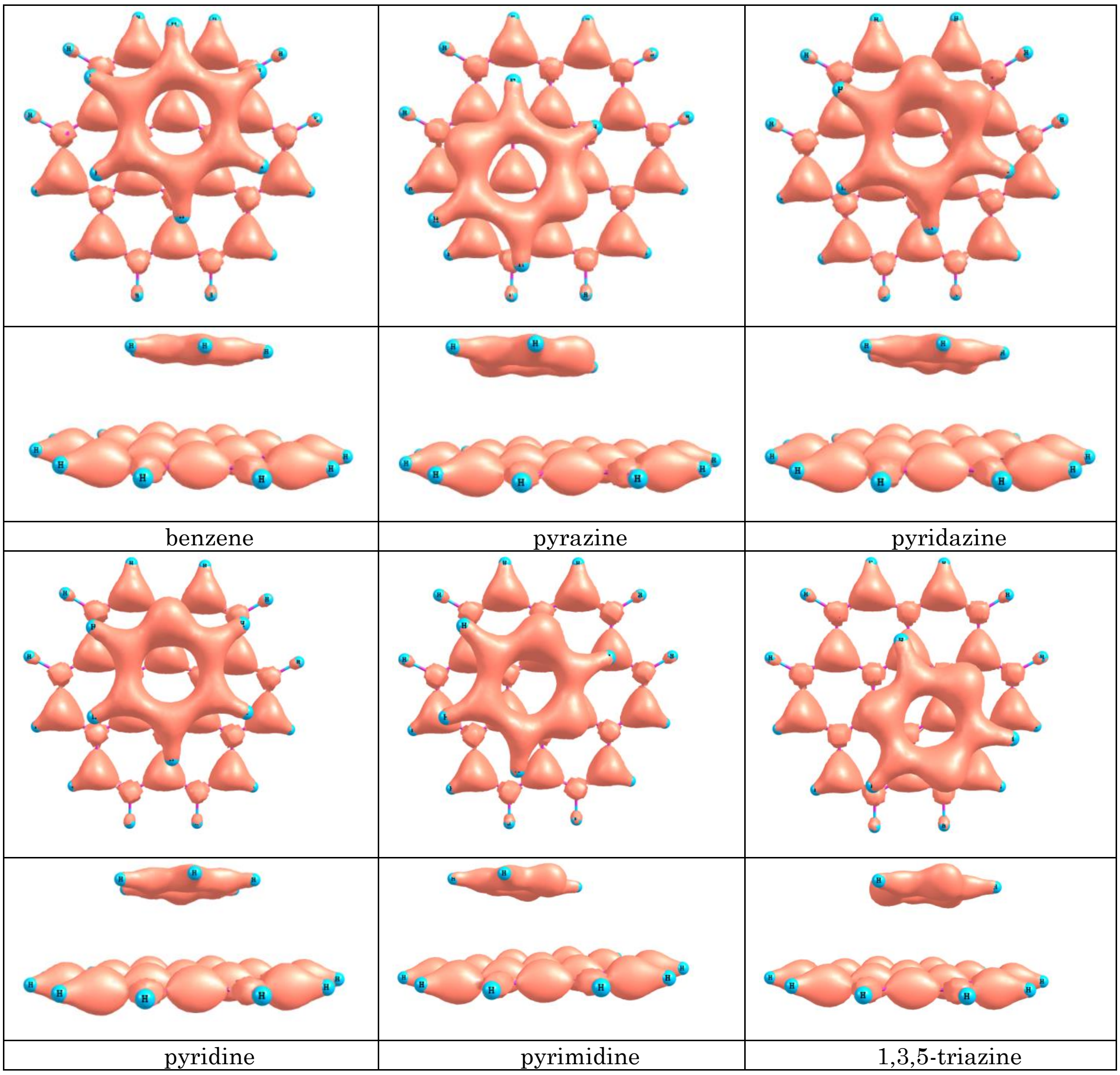

benzene | pyrazine | pyridazine

pyridine | pyrimidine | 1,3,5-triazine

Fig. 2 – Top: top view of electron density maps of molecule/*h*-BN complexes (isodensity = 0.2). Bottom: side view of electron density maps of molecule/*h*-BN complexes (isodensity = 0.2)

Table 1 – PBE-D3/SVP adsorption energies (E_a), equilibrium distances (R), dipole moments (μ), charge transfers (Δc), and HOMO-LUMO gaps (E_g) for studied complexes

System	E_a, eV	R, Å	μ, Debye	Δc^1, e	E_g, eV
h-BN	–	–	< 0.01^2	–	5.107
benzene/*h*-BN	– 0.304	3.33	0.00	0.028	4.778 (6.4 %)^3
pyrazine/*h*-BN	– 0.279	3.25	0.00	0.029	3.177 (37.8 %)
pyridazine/*h*-BN	– 0.315	3.27	3.95	0.034	2.621 (48.7 %)
pyridine/*h*-BN	– 0.317	3.30	2.09	0.029	3.925 (23.1 %)
pyrimidine/*h*-BN	– 0.286	3.34	2.19	0.019	3.516 (31.2 %)
1,3,5-triazine/*h*-BN	– 0.279	3.29	< 0.01	0.021	3.480 (31.9 %)

[1] Δc values were obtained as the difference between zero and the net Mulliken charge of the molecules adsorbed on *h*-BN. The positive Δc denotes the electron transfer to *h*-BN. [2] μ values are presented for individual molecules involved in this study. [3] The relative changes in E_g of *h*-BN are given in parentheses

values for the adsorption of pyridine onto graphene surface consisted of 24 carbon atoms: 0.250-0.311 eV [26]. These values are somewhat smaller than that derived in this study. For the benzene molecule, there exist the scattered results on E_a. Thus, for example, the work of Lechner and Sax using B3LYP-D2/def2-SVP gives the E_a value of 0.42 eV [27]. The paper of Berland and Hyldgaard, in turn, gives the E_a value of 0.49 for graphene and 0.48 eV for *h*-BN (the van der Waals density functional (VDW-DF1) calculation) [28]. The same work using VDW-DF2 calculations predicts the equal E_a values of 0.34 eV for both graphene and *h*-BN [28]. Ershova et al. using the dispersion corrected functional with various basis sets [29] show E_a of 0.47 and

0.37 eV for graphene. Wang et al. using ωB97X-D/def2-TZVPP level of theory yield E_a of 0.55 eV [6]. For the adsorption on graphene, Wuest and Rochefort predict the following E_a of 0.59, 0.60, 0.62 eV (PBE-D) for benzene, pyridine, and triazine, respectively [9]. Generally speaking, there are vast literature data on benzene adsorption. The information on azines is rather scarce, and we can only conclude that our calculations coincide well with the previously published results on benzene. The literature E_a values for the adsorption on graphene and *h*-BN are, generally, very close.

Now we turn to the adsorption on GBNCHs. Absolute E_a values obtained herein for all studied molecules are lower than those for the adsorption on GBNCHs (both studies use the same calculation method) [23]. We ascribe this result to the enhanced adsorption ability of GBNCH in comparison with *h*-BN. Indeed, the GBNCH model composed from different parts has increased number of polar C-B bonds at the interfacial region. It increases the following interactions: (i) permanent dipole (GBNCH)/permanent dipole (pyridazine, pyrimidine, or pyridine) or (ii) permanent dipole (GBNCH)/induced dipole (benzene, 1,3,5-triazine, or pyrazine).

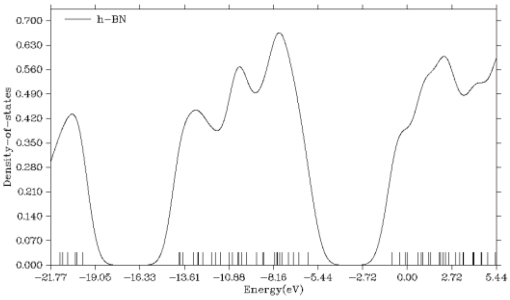

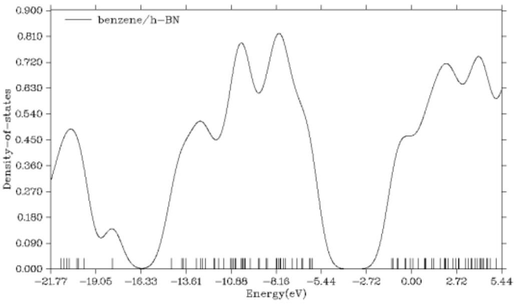

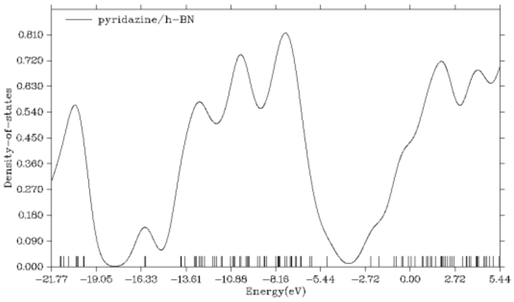

Fig. 3 – Density of states (DOS) plots for pristine *h*-BN (top) as well as benzene/*h*-BN (middle) and pyridazine/*h*-BN (bottom) complexes

To study the influence of adsorption on electronic properties of *h*-BN, we present the density of states (DOS) plots for pristine *h*-BN as well as benzene/*h*-BN and pyridazine/*h*-BN complexes, for the sake of comparison (Fig. 3). We can see that the shape of DOS plots for the complexes show only minor changes on attachment of different species, suggesting that that the physical adsorption of the studied molecules modifies weakly the electronic properties of *h*-BN. This conclusion can also be validated by the charge transfer (Δ*c*) between

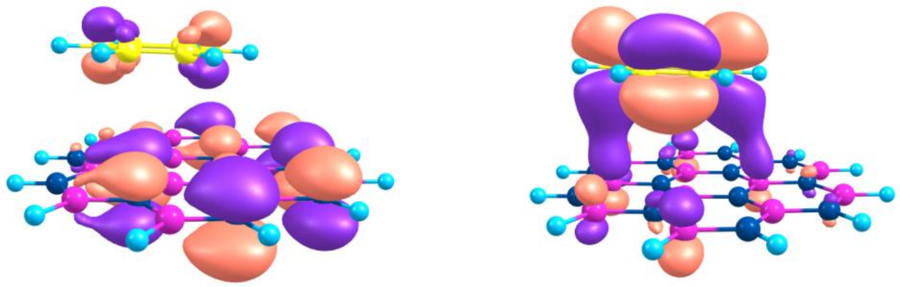

HOMO of benzene/h-BN complex LUMO of benzene/h-BN complex

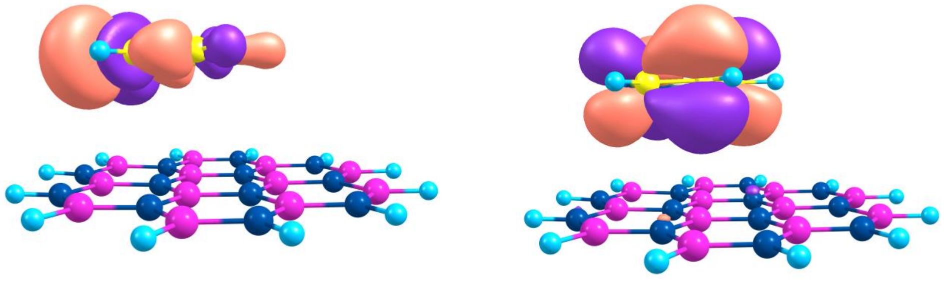

HOMO of pyridazine/h-BN complex LUMO of pyridazine/h-BN complex

Fig. 4 – HOMO and LUMO (isodensity = 0.03) of benzene/*h*-BN and pyridazine/*h*-BN complexes

the N-containing heterocycles and *h*-BN (Table 1). Indeed, one can note that the Δ*c* values are small. Nevertheless, the new states occur near the highest occupied (HOMO) and the lowest unoccupied molecular orbitals (LUMO) (Fig.3, the DOS plot for the pyridazine/*h*-BN complex, vertical bars near the HOMO and LUMO). These peculiarities are inherent for all N-containing heterocycles studied herein (their DOS plots are not presented) that leads to the substantial changes in E_g of studied complexes compared with the pristine *h*-BN (Table 1). At the same time, the physisorption of benzene introduces very little changes in the E_g value of *h*-BN (Table 1).

The shapes of the HOMO and LUMO of studied complexes can qualitatively approve our findings (Fig. 4). The HOMO and LUMO for the pyridazine/*h*-BN complex have the main input from the pyridazine molecule. This substantial contribution leads to the large changes in E_g (Table 1). Conversely, the HOMO and LUMO for the benzene/*h*-BN complex are contributed by the *h*-BN in the larger extent, whereas the input of the benzene molecule to these orbitals is smaller than that in the case of pyridazine (Fig. 4). Therefore, the changes in E_g of the benzene/*h*-BN complex are minor compared with heterocycle/*h*-BN ones (Table 1).

4. CONCLUSION

All in all, we perform DFT-D3 calculations to study the physical adsorption of a series of five N-containing heterocycles, and, for the sake of comparison, a benzene molecule on *h*-BN. The difference in E_a for all studied molecules can be explained by the magnitude of their dipole moments. The larger values of μ correspond to larger E_a, which vary from 0.279 to 0.317 eV. Among studied molecules, those with the non-zero μ values exhibit maximal E_a. For the non-polar molecules, only one non-specific interaction (permanent dipole-induced dipole) holds which leads to smaller E_a. For polar molecules, the additional term corresponding to the field-dipole interactions arises. Except pyridazine, the physisorption of all the molecules on *h*-BN, results in little changes in its electronic structure, representing a simple method to add arbitrary functionality to *h*-BN, preserving its electronic properties practically undisturbed.

ACKNOWLEDGEMENTS

This work was partially supported by the base part of the Government Assignment for Scientific Research from the Ministry of Education and Science of Russia (project code: 13.7232.2017/8.9). Generous allotment of computational time from Computational Center of Novosibirsk State University (www.nusc.ru) is gratefully acknowledged. The authors thank the joint center “Baikal Center of Nanotechnologies” for its facilities.

Физическая адсорбция азотсодержащих гетероциклов на гексагональном нитриде бора: исследование методом функционала плотности

И.К. Петрушенко

Иркутский национальный исследовательский технический университет, ул. Лермонтова, 83, 664074 Иркутск, Россия

В настоящей работе была изучена физисорбция пяти различных азотсодержащих органических гетероциклических молекул и бензола на гексагональном нитриде бора (*h*-BN) с использованием дисперсионно-скорректированной теории функционала плотности (DFT-D3). Энергии адсорбции (E_a) были определены для всех изучаемых молекул, и было показано, что E_a для пиридазина является максимальной. Также получены электронные свойства комплексов молекула/*h*-BN. Расчеты методом DFT-D3 показывают, что все исследуемые молекулы, за исключением пиридазина, вводят лишь незначительные изменения в энергетический зазор ВЗМО-НСМО *h*-BN при физисорбции. Таким образом, физисорбция азотсодержащих молекул на плоскости *h*-BN посредствои нековалентных ван-дер-ваальсовых взаимодействий представляет собой простой способ для добавления произвольной функциональности к *h*-BN с сохранением их электронных свойств. Кроме того, было проведено сравнение величин E_a для адсорбции на графене, *h*-BN и их гибридной структуре.

Ключевые слова: DFT, Гексагональный нитрид бора, Азот, Гетероцикл, Физисорбция, Графен.

REFERENCES

1. K.S. Novoselov, A.K. Geim, S.V. Morozov, D. Jiang, Y. Zhang, S.V. Dubonos, I.V. Grigorieva, A.A. Firsov, *Science* **306**, 666 (2004).
2. W. Hu, N. Xia, X. Wu, Z. Li, J. Yang, *Phys. Chem. Chem. Phys.* **16**, 6957 (2014).
3. M. Kawaguchi, S. Kuroda, Y. Muramatsu, *J. Phys. Chem. Solids* **69**, 1171 (2008).
4. Q. Tang, Z. Zhou, Z. Chen, *Wires Comput. Mol. Sci.* **5**, 360 (2015).
5. S. Zhao, J. Xue, *J. Phys. D Appl. Phys.* **46**, 135303 (2013).
6. W. Wang, Y. Zhang, Y.-B. Wang, *J. Chem. Phys.* **140**, 094302 (2014).
7. W. Chen, S. Chen, D.C. Qi, X.Y. Gao, A.T.S. Wee, *J. Am. Chem. Soc.* **129**, 10418 (2007).
8. Z. Zhang, H. Huang, X. Yang, L. Zang, *J. Phys. Chem. Lett.* **2**, 2897 (2011).
9. J.D. Wuest, A. Rochefort, *Chem. Commun.* **46**, 2923 (2010).
10. L. Kong, A. Enders, T.S. Rahman, P.A. Dowben, *J. Phys-Condens. Mat.* **26**, 443001 (2014).
11. G.D. Henry, *Tetrahedron* **60**, 6043 (2004).
12. F. Neese, *Wires Comput. Mol. Sci.* **2**, 73 (2012).
13. S. Grimme, *J. Comput. Chem.* **27**, 1787 (2006).
14. S. Grimme, J. Antony, S. Ehrlich, H. Krieg, *J. Chem. Phys.*

132, 154104 (2010).
15. S. Grimme, S. Ehrlich, L. Goerigk, *J. Comput. Chem.* **32**, 1456 (2011).
16. J.P. Perdew, K. Burke, M. Ernzerhof, *Phys. Rev. Lett.* **77**, 3865 (1996).
17. J.P. Perdew, K. Burke, M. Ernzerhof, *Phys. Rev. Lett.* **78**, 1396 (1997).
18. H.H. Ansgar Schafer, R. Ahlrichs, *J. Chem. Phys.* **97**, 2571 (1992).
19. M. Moradi, M. Nouraliei, R. Moradi, *Physica E* **87**, 186 (2017).
20. I.K. Petrushenko, K.B. Petrushenko, *Int. J. Hydrogen Ener.* **43**, 801 (2018).
21. J. Beheshtian, A.A. Peyghan, M.B. Tabar, Z. Bagheri, *Appl. Surf. Sci.* **266**, 182 (2013).
22. T. Lu, F. Chen, *J. Comput. Chem.* **33**, 580 (2012).
23. I.K. Petrushenko, K.B. Petrushenko, *Comput. Theor. Chem.* **1117**, 162 (2017).
24. P.-P. Zhou, R.-Q. Zhang, *Phys. Chem. Chem. Phys.* **17**, 12185 (2015).
25. R.T. Yang, *Adv. Chem. Eng.* **27**, 79 (2001).
26. N. Ramos-Berdullas, I. Perez-Juste, C. Van Alsenoy, M. Mandado, *Phys. Chem. Chem. Phys.* **17**, 575 (2015).
27. C. Lechner, A.F. Sax, *J. Phys. Chem. C* **118**, 20970 (2014).
28. K. Berland, P. Hyldgaard, *Phys. Rev. B* **87**, 205421 (2013).
29. O.V. Ershova, T.C. Lillestolen, E. Bichoutskaia, *Phys. Chem. Chem. Phys.* **12**, 6483 (2010).